UC Berkeley

UC Berkeley Previously Published Works

Title
Precision Engineering of 2D Protein Layers as Chelating Biogenic Scaffolds for Selective
Recovery of Rare-Earth Elements

Authors
Pallares, Roger M
Charrier, Marimikel
Tejedor-Sanz, Sara
et al.

Article

Precision Engineering of 2D Protein Layers as Chelating Biogenic Scaffolds for Selective Recovery of Rare-Earth Elements

Roger M. Pallares, Marimikel Charrier, Sara Tejedor-Sanz, Dong Li, Paul D. Ashby, Caroline M. Ajo-Franklin,* Corie Y. Ralston,* and Rebecca J. Abergel*

Read Online

ACCESS | Metrics & More | Article Recommendations | Supporting Information

ABSTRACT: Rare-earth elements, which include the lanthanide series, are key components of many clean energy technologies, including wind turbines and photovoltaics. Because most of these 4f metals are at high risk of supply chain disruption, the development of new recovery technologies is necessary to avoid future shortages, which may impact renewable energy production. This paper reports the synthesis of a non-natural biogenic material as a potential platform for bioinspired lanthanide extraction. The biogenic material takes advantage of the atomically precise structure of a 2D crystalline protein lattice with the high lanthanide binding affinity of hydroxypyridinonate chelators. Luminescence titration data demonstrated that the engineered protein layers have affinities for all tested lanthanides in the micromolar-range (dissociation constants) and a higher binding affinity for the lanthanide ions with a smaller ionic radius. Furthermore, competitive titrations confirmed the higher selectivity (up to several orders of magnitude) of the biogenic material for lanthanides compared to other cations commonly found in f-element sources. Lastly, the functionalized protein layers could be reused in several cycles by desorbing the bound metal with citrate solutions. Taken together, these results highlight biogenic materials as promising bioadsorption platforms for the selective binding of lanthanides, with potential applications in the recovery of these critical elements from waste.
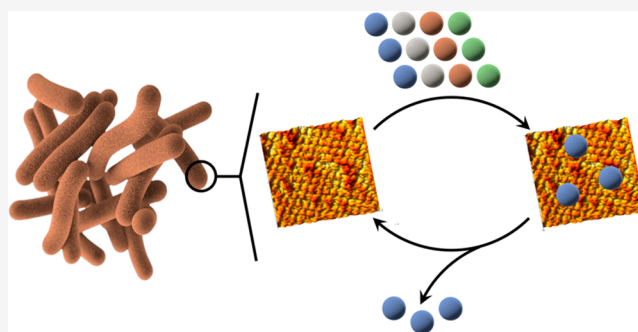
INTRODUCTION

Clean energy generation through wind turbines and photovoltaics requires metals with a high risk for supply chain disruption.[1] Among those critical metals, the U.S. Department of Energy (DOE) has highlighted eight lanthanides (lanthanum, cerium, praseodymium, neodymium, samarium, europium, terbium, and dysprosium)[2] for which new strategies for recovery and reuse are direly needed. Current industrial separation processes of lanthanides from waste involve solvent extraction, where hydrophobic molecules extract the cations into an organic liquid phase,[3,4] or ion exchange, where the metal chelated by a ligand interacts with a solid phase, such as functionalized resins.[5,6] These separation strategies, however, tend to generate large quantities of acidic waste. Moreover, most commercially available chelating ligands, such as ethylenediaminetetraacetic acid, are nonselective toward lanthanides, resulting in low-efficiency separation processes.[7] Recent discoveries on natural lanthanide-binding proteins, such as lanmodulin[8,9] and enzyme cofactor PQQ,[10] as well as designed de novo proteins[11,12] have brought attention toward bioinspired lanthanide extraction strategies. These proteins can display extremely high binding affinities for f-elements; however, their applications for large scale extraction or the separation of each lanthanide from one another are expected to

be challenging. Therefore, strategies that exploit more readily accessible and tunable bioinspired materials would be highly beneficial for the recovery and purification of rare-earth elements.

Surface layers (S-layers) are two-dimensional crystalline arrays of proteins that constitute an external part of the cell envelope of many bacteria and nearly all archaea.[13] Because of their high-density display, well-defined symmetry, and spacing, S-layers have been used as scaffolds for a wide range of applications, such as catalysis, therapeutics, and sensing.[14−16] To date, the structures of only a few S-layer proteins have been atomically resolved, including those of SbsB (from *Geobacillus stearothermophilus* PV72)[17] and RsaA (from *Caulobacter crescentus* CB15).[18] This structural information has allowed for the genetic modification of both SbsB[19] and RsaA,[20] so that biomolecules and nanomaterials can be attached in precise, repeating locations across the 2D lattice. One aspect of interest
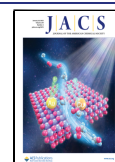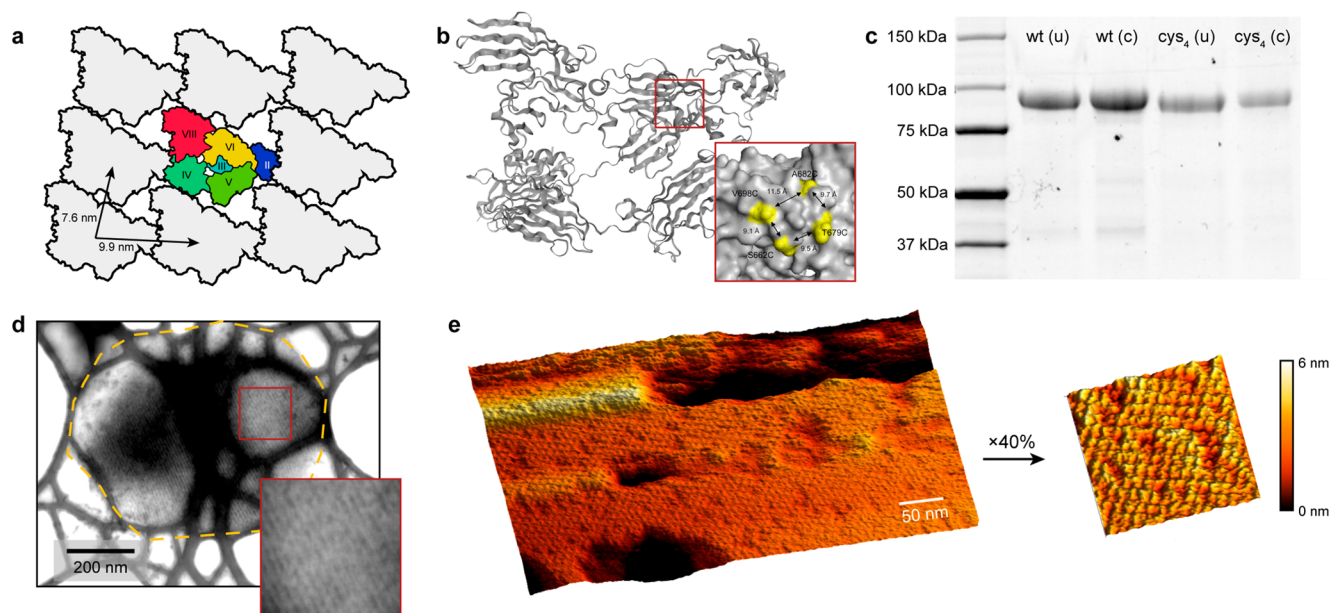
Figure 1. (a) Scheme of the SbsB S-layer with the protein domains highlighted in color. (b) Structure of the SbsB protein with the positions modified with cysteines highlighted in yellow. (c) Sodium dodecyl sulfate polyacrylamide gel electrophoresis (SDS-PAGE) immunoblot of wild-type (wt) and four cysteine-modified (cys$_4$) SbsB before and after His-tag cleavage (indicated as "u" and "c" for uncleaved and cleaved protein, respectively). (d) Scanning transmission electron microscopy (STEM) and (e) high-resolution atomic force microscopy (HR-AFM) height images of SbsB protein S-layers modified with four cysteines. The STEM sample was imaged in holey carbon film with a Cu grid, and the S-layer profile is highlighted with a yellow dashed line for clarity.

for such modifications is the demonstrated potential of engineered S-layers and other surface-displayed proteins to render bacterial cells more specific as metal biosorbents. Bacteria display a variety of chemical groups that permit nonspecific biosorption of metals and other pollutants from waters and soils, since they can be more efficient than commercial adsorbents.[21] To enhance their selectivity, surface modifications through bioengineering and chemical methods have been developed,[21] including for instance, the functionalization of S-layers with metal-binding units, leading to a higher selectivity toward heavy metals.[22,23] However, those biogenic materials have been primarily focused on the extraction of metals from the d-block. Recently, bacteria have been engineered to display lanthanide-binding tags, short peptides that show high affinity for lanthanides, resulting in a higher binding selectivity toward those rare-earth elements and good separation performance.[24,25] Nevertheless, lanthanide-binding tags have low affinity for lanthanides in acidic conditions, particularly below pH 4.5, limiting their application during separations of acidic leachates. Ligands containing bidentate hydroxypyridinonate (HOPO) moieties are good alternatives to lanthanide-binding tags, since they show high binding affinity and selectivity for f-block elements, and they can be quantitively bind to the f-elements even in strong acid conditions.[26,27] Although HOPO-based ligands have been widely used in separation,[28,29] decorporation,[30−32] therapeutics,[33] and detection,[34,35] they have not been incorporated yet into biogenic materials. A biosorbent technology that combines the well-ordered two-dimensional structure of S-layers with the high affinity of HOPO units for lanthanides would represent an advancement in the separation and extraction of these metals from waste waters.

Here, we report the synthesis of a non-natural biogenic material constituted by engineered SbsB S-layers and HOPO

binding units for the selective bioadsorption of lanthanides. SbsB S-layers were engineered to display four cysteine residues per monomer, which were used as attachment points for the HOPO moieties. The binding capabilities of the resulting HOPO$_4$−SbsB S-layers were evaluated through spectrofluorimetric titrations. The dissociation constants (K_D) were determined to be in the micromolar-range for all tested lanthanides, with the S-layer showing a higher binding affinity for those lanthanides with a smaller ionic radius. Furthermore, competitive titrations confirmed the higher selectivity of HOPO$_4$−SbsB for lanthanides compared to other metal ions commonly found in f-element sources. Lastly, HOPO$_4$−SbsB could be reused in multiple cycles by employing a biocompatible desorbing agent, such as sodium citrate.

■ RESULTS AND DISCUSSION

Engineering SbsB S-Layers to Display HOPO Ligands. S-layers made of SbsB proteins were chosen as scaffolds for the biogenic material because of their highly symmetrical structure (Figure 1a), ease of expression and modification, and lack of cysteines in the wild-type sequence. The SbsB expression and purification was performed in *Escherichia coli* following a modified version of a previous published protocol,[36] which included the use of cleavable polyhistidine tags (His-tags, Figure S1).[37] We previously engineered SbsB proteins to incorporate cysteines,[19] which we used in this work as surface covalent attachment points for the HOPO chelating units. Because siderophore-derived ligands require four HOPO subunits to maximize their affinity for lanthanides,[26] we chose a strain with four superficial cysteines (forming an ∼1 nm × ∼1 nm square), which in our previous work was used to bind gold nanoparticles on the surface of the S-layer.[19] The cysteine locations within the protein were selected on the basis of their relative proximity and surface accessibility (Figure 1b).
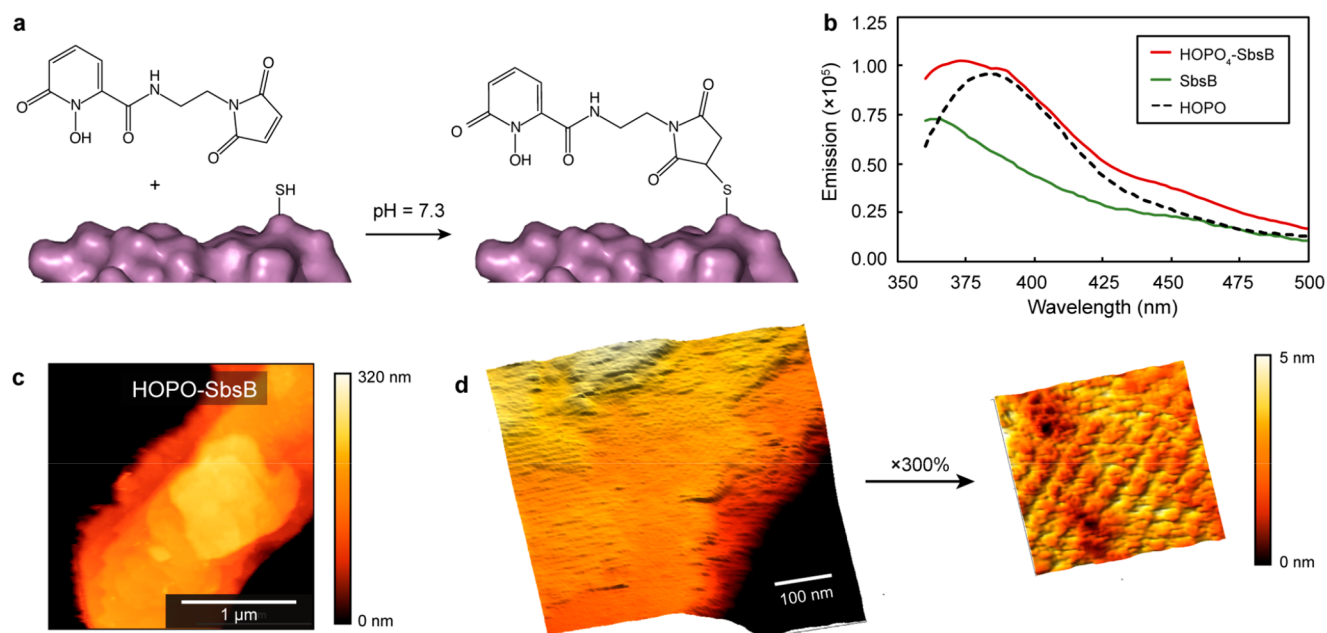
Figure 2. (a) Scheme of the coupling reaction between HOPO chelate and cysteine-modified SbsB. (b) Emission spectra of SbsB coupled with HOPO (HOPO$_4$–SbsB), SbsB, and HOPO after excitation at 315 nm. (c) HR-AFM height image of HOPO$_4$–SbsB flakes. (d) HR-AFM images of HOPO$_4$–SbsB periodic structure.

Immunoblot analysis showed bands at ∼96 kDa for the wild-type protein (wt-SbsB), in agreement with previously reported data,[37] and for the modified SbsB with four cysteines (cys$_4$-SbsB) before and after the His-tag cleavage (Figure 1c). Confocal microscopy (Figure S2a,2b) confirmed that both wild-type and cysteine-modified SbsB formed S-layer sheets. The cysteine-modification did not disrupt the formation of the lattice structure in the S-layers, as observed by scanning transmission electron microscopy (STEM, Figure 1d) and high-resolution atomic force microscopy (HR-AFM, Figure 1e). Furthermore, HR-AFM line profile analysis showed that both wt-SbsB and cys$_4$-SbsB had crystalline lattice structures with 10 nm repeating lengths (Figure S3), further confirming that cys$_4$-SbsB retains the nanoscale structure of native SbsB.

The siderophore-inspired 3,4,3-LI(1,2-HOPO) chelator has shown a high affinity for f-block elements under a wide range of experimental conditions.[26,38−40] Hence, we chose the HOPO subunits from this archetype ligand as metal binding moieties for the biogenic material. The HOPO units conjugated with maleimide groups (Figure S4) were coupled to the SbsB cysteines through maleimide coupling at pH 7.3 for 5 h (Figure 2a). To ensure the functionalization of all cysteines, a 50-fold excess of chelator to cysteine was used. After washing three times, luminescence spectroscopy of the S-layers showed the presence of both SbsB and HOPO units (Figure 2b), which confirmed that the coupling between the cysteines and the maleimide-terminated chelating units was successful. A functionalization yield of ∼95% was estimated by labeling the remaining free cysteines (after HOPO functionalization) with Cy3-maleimide dye (Figure S5). After the functionalization with HOPO, the S-layers remained as 2D sheets (Figure 2c and Figure S2c), and their crystalline lattice structure (Figure 2d) with the characteristic 10 nm repeating length was preserved, as shown by HR-AFM line profile analysis (Figure S3).

Selective Binding of Lanthanides to the Engineered S-Layer. We first explored the binding between lanthanides and HOPO-functionalized SbsB layers (HOPO$_4$–SbsB) using Eu^{3+} since it is one of the critical elements highlighted by the U.S. DOE and its luminescence can be sensitized by HOPO moieties. Hence, we assessed the binding of Eu^{3+} to the S-layer surface through direct spectrofluorimetric titration. Different concentrations of metal (from 0 to 180 μM) were added to 30 μg/mL S-layer solutions (0.3 μM, either HOPO$_4$–SbsB or wt-SbsB) at pH 6.0. This pH was selected because it is commonly used during rare-earth element recovery with biomaterial-based protocols, as it is low enough to prevent metal precipitation in the form of oxides but not acidic enough to damage most biomaterials.[24,25] After a 15 min incubation period at room temperature, the solution emissions were recorded under excitation at 315 nm (i.e., the position of the HOPO absorption band maximum). An emission band centered at 622 nm, which is characteristic of Eu^{3+},[34,38] was observed after the addition of the metal to the HOPO$_4$–SbsB solutions (Figure 3a). As the concentration of Eu^{3+} increased, so did the emission intensities of the HOPO$_4$–SbsB solutions, confirming the binding between the metal and the HOPO moieties. In the case of wt-SbsB solutions, no emission band was observed after the addition of Eu^{3+} (Figure 3b). The distinct behaviors of HOPO$_4$–SbsB and wt-SbsB are clearly observed in Figure 3c. A dissociation constant (K_D) for the binding of Eu^{3+} to HOPO$_4$–SbsB at pH 6.0 of 22.6 ± 1.6 μM was determined with the titration data (Figure S6). A Hill coefficient of 1 was obtained with the titration data, likely reflecting the binding of one Eu^{3+} ion to the four HOPO units. This is the same stoichiometry that has been reported for the binding between lanthanides and other HOPO-based ligands.[26,28] It is worth noting that K_D values are pH dependent, as they are affected by both protonation of the ligand and speciation/precipitation of the metal.[41] Similar results were obtained for spectrofluorimetric titrations using
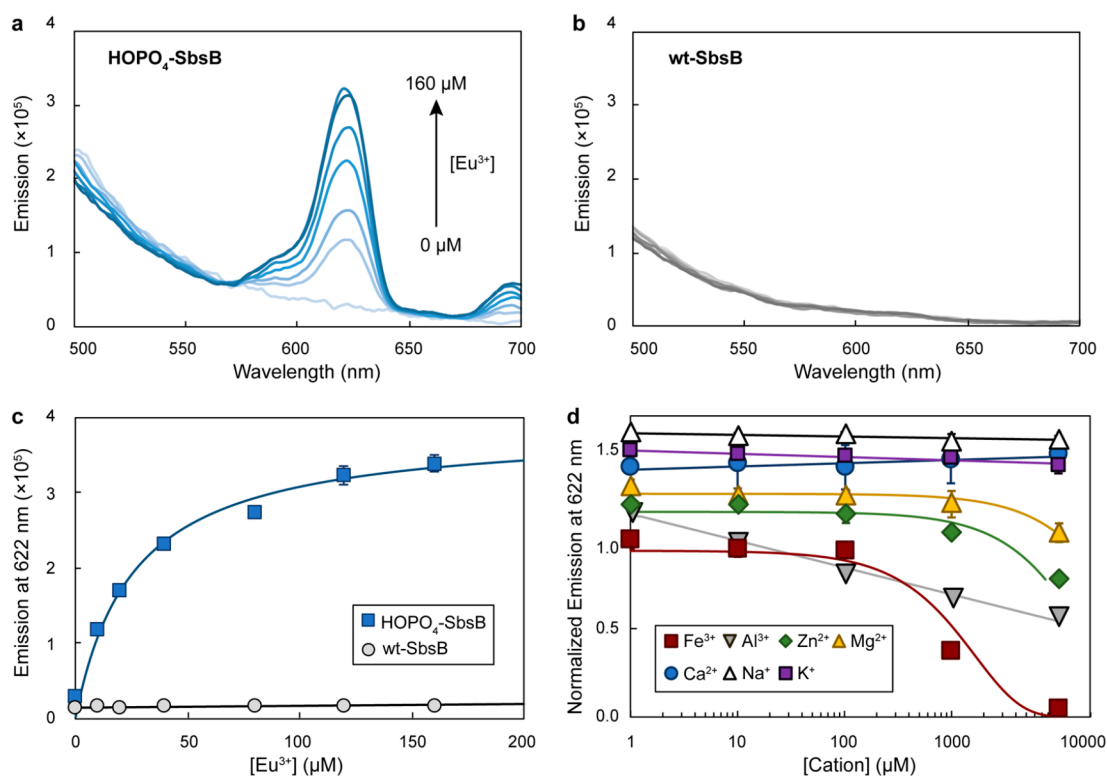
Figure 3. Emission spectra of (a) HOPO$_4$−SbsB or (b) wt-SbsB (0.3 μM) after the addition of different amounts of Eu^{3+} (from 0 to 160 μM). (c) Emission at 622 nm after the addition of Eu^{3+}. (d) Normalized emission at 622 nm after the addition of Fe^{3+}, Al^{3+}, Zn^{2+}, Mg^{2+}, Ca^{2+}, K$^+$, or Na$^+$ to solutions containing HOPO$_4$−SbsB (0.3 μM) and Eu^{3+} (80 μM). The curves have been offset for clarity. All experiments were performed at pH 6.0 (0.375 M MES). The excitation wavelength for all measurements was 315 nm.

280 nm excitation (wavelength used to excite tyrosine and tryptophan residues), in which solutions containing HOPO$_4$−SbsB and Eu^{3+} showed emission while solutions containing wt-SbsB and Eu^{3+} did not (Figure S7). The emission intensities of the HOPO$_4$−SbsB solutions, however, were lower when exciting at 280 nm compared to 315 nm, suggesting that the energy transfer between the amino acids and the metal was a less efficient process compared to the energy transfer between HOPO units and Eu^{3+}. Taken together, these results indicate that the binding between the HOPO moieties and Eu^{3+} occurs near tyrosine and tryptophan residues. In the case of the wt-SbsB, the results suggest that there is no metal binding near any of these two types of amino acids. Although 280 nm excitation only sensitizes metal ions near tyrosine and tryptophan residues, SbsB contains over 20 tyrosine and 3 tryptophan residues spread throughout its structure (Figure S8). Hence, these measurements can provide qualitative information regarding the nonspecific binding of Eu^{3+} to the S-layer.

Because lanthanides are mixed with other metals in waste and natural ores, we assessed Eu^{3+} binding to HOPO$_4$−SbsB in the presence of other cations commonly found in source materials. Competitive spectrofluorimetric titrations were carried out by adding increasing amounts of competing metals to solutions made of HOPO$_4$−SbsB (0.3 μM) and Eu^{3+} (80 μM). As Eu^{3+} was displaced from the HOPO moieties by the competing metals, its luminescence decreased (Figure 3d). Nevertheless, HOPO$_4$−SbsB displayed a higher selectivity toward Eu^{3+} compared to the tested metals. For instance, additions of up to 1 mM of competing cations (1 order of magnitude higher than Eu^{3+}) did not affect the Eu^{3+} binding, as

the luminescence of the samples remained constant, except for Fe^{3+} and Al^{3+}, which decreased the sample emissions by 63 ± 1% and 34 ± 1% after the addition of 1 mM Fe^{3+} and Al^{3+}, respectively. Overall, these experiments confirmed the higher selectivity of HOPO$_4$−SbsB for Eu^{3+} compared to other metal ions commonly found in natural and anthropogenic sources of lanthanides.

We also studied the effect of pH on the binding between the functionalized S-layer and Eu^{3+}. All samples containing Eu^{3+} and HOPO$_4$−SbsB showed emission at 622 nm from pH 4 to 7, indicating metal binding (Figure S9). The emission intensities decreased as the acidity of the solution increased. These results were consistent with a previous publication that characterized the emission of Eu^{3+} with 3,4,3-LI(1,2-HOPO), the corresponding octadentate ligand architecture. Although most Eu^{3+} was complexed by 3,4,3-LI(1,2-HOPO) at any point from pH 2 to 8, a decrease in emission intensity was observed as acidity increased, due to the protonation of the HOPO units.[38] Because some key biomaterials used for rare-earth element recovery lose most metal binding capabilities at pH 5,[24,25] we further performed a spectrofluorimetric titration at such a low pH (Figure 4a). As previously observed, the emission intensities of the samples were 1 order of magnitude lower at pH 5.0 compared to the same samples at pH 6.0 (Figure 4b). To better understand the impact of pH in our system, we determined the K_D of the binding at pH 5.0 using the titration data (Figure S10). Decreasing the pH from 6.0 to 5.0 resulted in an increase of the K_D from 22.6 ± 1.6 to 43.7 ± 14.1 μM. Hence, although increasing the solution acidity decreased the binding affinity between HOPO$_4$−SbsB and Eu^{3+}, the K_D values at both pH were in the micromolar-range,
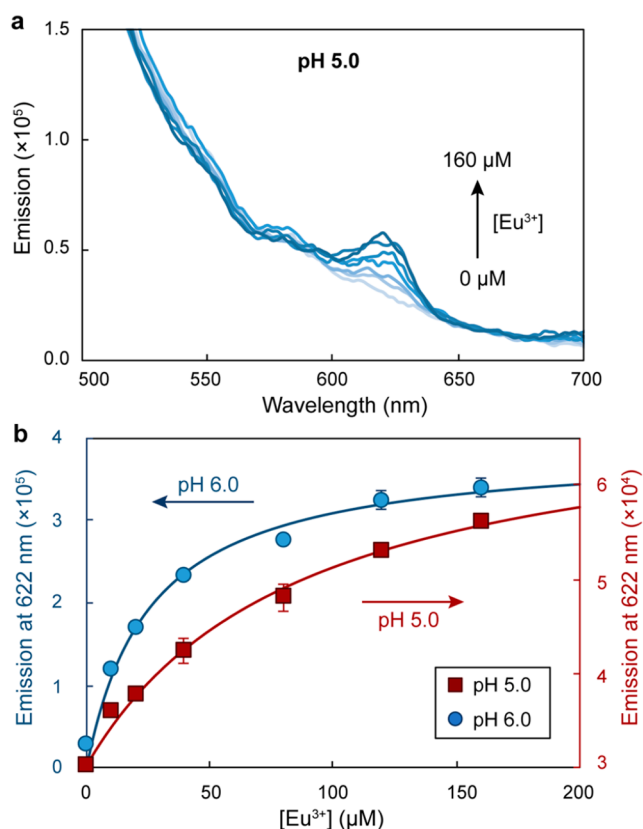
Figure 4. (a) Emission spectra of HOPO$_4$−SbsB (0.3 μM) after the addition of different amounts of Eu^{3+} (from 0 to 160 μM) at pH 5.0 (0.375 M acetate buffer). (b) Emission at 622 nm after the addition of Eu^{3+} at pH 5.0 or 6.0. The excitation wavelength for all measurements was 315 nm.

Figure 5. Normalized emission at 622 nm after the addition of La^{3+}, Ce^{3+}, Pr^{3+}, Dy^{3+}, or Ho^{3+} to solutions containing HOPO$_4$−SbsB (0.3 μM) and Eu^{3+} (80 μM). The curves have been offset for clarity. All experiments were performed at pH 6.0 (0.375 M MES). The excitation wavelength for all measurements was 315 nm.

Table 1. Summary of Equilibrium Dissociation Constants (K_D) for HOPO$_4$−SbsB and Lanthanide Complexes Measured at pH 6.0

lanthanide	K_D (μM)
La^{3+}	452.8 ± 121.0
Ce^{3+}	72.7 ± 5.7
Pr^{3+}	26.0 ± 2.7
Eu^{3+}	22.6 ± 1.6
Dy^{3+}	10.0 ± 1.6
Ho^{3+}	9.0 ± 0.6

highlighting the good affinity of the HOPO-moieties for the metal.

Next, we assessed the binding selectivity of HOPO$_4$−SbsB for different lanthanides. It is noteworthy that discriminating lanthanides is very challenging because of their consistent properties, such as a similar ionic size and preference for the +3-oxidation state.[42] Thus, a biogenic material that displays distinct binding affinities across the series would be highly beneficial for not only lanthanide recovery but also separation. Spectrofluorimetric titrations were performed by adding increasing amounts of competing lanthanides (e.g., La^{3+}, Ce^{3+}, Pr^{3+}, Dy^{3+}, and Ho^{3+}) to solutions made of HOPO$_4$−SbsB (0.3 μM) and Eu^{3+} (80 μM). Because the luminescence of the competing lanthanides was not sensitized by the HOPO moieties, Eu^{3+} displacement from the functionalized S-layer could be tracked by the decrease of its luminescence (Figure 5). The titration data was used to determine the K_D of the different lanthanides (Table 1), which ranged from 9.0 ± 0.6 (Ho^{3+}) up to 452.8 ± 121.0 μM (La^{3+}). These values were in the same range (slightly higher) as those previously reported for S-layers modified with lanthanide binding tags.[24,25] Our system, however, preserved the binding affinity at pH 5.0, while previous systems lost the majority of their metal-binding capabilities at such a low pH.[24,25]

The K_D values were over 30-fold larger than the protein concentration used during the titrations. Hence, the titrations were performed under a binding regime, and the values were determined under adequate conditions.[43] Considering overall trends, the binding affinities increased (decreasing K_D values) across the lanthanide series, with up to 2 orders of magnitude difference between La and Ho. This effect is similar to but less pronounced than that observed with the archetype octadentate ligand 3,4,3-LI(1,2-HOPO).[26] This trend is usually attributed to a combination of the decreasing cation radii size and the increasing metal's Lewis acidity when progressing throughout the 4f series. However, it may be less prominent for the protein structure than for the small molecule analogue, as there is more accessibility in the latter to accommodate water molecules within the complex inner sphere, thereby amplifying differences in coordination numbers. In contrast, a large macromolecular structure may shield the immediate vicinity of the metal center from additional coordinating water molecules.

Lastly, we designed a strategy to recycle the functionalized S-layers in order to reuse them for multiple extraction cycles. Hence, we performed several cycles of Eu^{3+} binding and desorption from the HOPO$_4$−SbsB, tracking the metal binding by measuring the emission intensity at 622 nm. To promote the release of the Eu^{3+}, we employed sodium citrate, a biocompatible chemical commonly used for metal desorption from surfaces[25] (for details about the experiment refer to the experimental section in the Supporting Information). As shown in Figure 6, the Eu^{3+} binding to the functionalized S-layer was reversible; it was also rapid, as equilibrium was reached within a few minutes for each measurement. Furthermore, the binding capacity of the HOPO$_4$−SbsB was preserved after using the citrate solution. Therefore, these results indicate that our biogenic material can be reused in multiple extraction cycles.

Although the HOPO$_4$−SbsB layers can be used directly as biosorbent substrates for lanthanide recovery and recycle, we
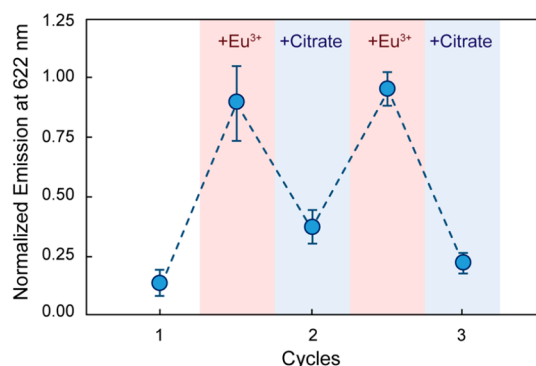
Figure 6. Normalized emission at 622 nm after the addition of Eu^{3+} (80 μM) or sodium citrate (50 mM) to solutions containing $HOPO_4$–SbsB (0.3 μM). All measurements were performed at pH 6.0 (0.375 M MES). The excitation wavelength for all measurements was 315 nm.

envision (and are currently working on) engineering live bacteria, which would display $HOPO_4$–SbsB on their surface. Hence, films of bacteria exposed to lanthanide-rich solutions could be used to recover the metals, which then could be desorbed from the S-layers by citrate treatments.

CONCLUSIONS

In summary, we have developed a biogenic material that selectively binds to lanthanides by combining SbsB S-layers and HOPO moieties. The proteins were engineered to display four cysteine residues that were later used to attach the HOPO binding units. The resulting $HOPO_4$–SbsB preserved the two-dimensional crystalline structure of the S-layer, as well as the high binding affinity of HOPO ligands for f-elements (K_D for all tested lanthanides were in the micromolar-range). In addition, the $HOPO_4$–SbsB layers were selective toward lanthanides, withstanding the presence of competing metals with concentrations up to 1 order of magnitude greater than Eu^{3+} without affecting the lanthanide binding to the HOPO unit. Lastly, $HOPO_4$–SbsB could be reused in several cycles by desorbing the bound metal with citrate solutions. All these results indicate that the functionalized S-layer is a promising and reusable bioadsorption platform for selective lanthanide binding with potential applications in the recovery of these critical metals from waste.

ASSOCIATED CONTENT

ⓈⒾ Supporting Information

The Supporting Information is available free of charge at https://pubs.acs.org/doi/10.1021/jacs.1c10802.

Discussions of experimental details, figures of immuno-blot image, confocal microscopy images, HR-AFM height images, line profile analysis, LC–MS analysis, emission spectra, Hill plot, structure of SbsB, and emission of $HOPO_4$-SbsB and wt-SbsB, and table of strains used (PDF)

AUTHOR INFORMATION

Corresponding Authors

Caroline M. Ajo-Franklin − *Molecular Foundry, Lawrence Berkeley National Laboratory, Berkeley, California 94720, United States; Department of BioSciences, Rice University,* Houston, Texas 77005, United States; ⓞ orcid.org/0000-0001-8909-6712; Email: cajo-franklin@rice.edu

Corie Y. Ralston − *Molecular Foundry, Lawrence Berkeley National Laboratory, Berkeley, California 94720, United States;* ⓞ orcid.org/0000-0002-7899-0951; Email: cyralston@lbl.gov

Rebecca J. Abergel − *Chemical Sciences Division, Lawrence Berkeley National Laboratory, Berkeley, California 94720, United States; Department of Nuclear Engineering, University of California, Berkeley, California 94720, United States;* ⓞ orcid.org/0000-0002-3906-8761; Email: abergel@berkeley.edu

Authors

Roger M. Pallares − *Chemical Sciences Division, Lawrence Berkeley National Laboratory, Berkeley, California 94720, United States;* ⓞ orcid.org/0000-0001-7423-8706

Marimikel Charrier − *Molecular Foundry, Lawrence Berkeley National Laboratory, Berkeley, California 94720, United States;* ⓞ orcid.org/0000-0003-4264-5985

Sara Tejedor-Sanz − *Molecular Foundry, Lawrence Berkeley National Laboratory, Berkeley, California 94720, United States;* ⓞ orcid.org/0000-0002-1192-8256

Dong Li − *Molecular Foundry, Lawrence Berkeley National Laboratory, Berkeley, California 94720, United States*

Paul D. Ashby − *Molecular Foundry, Lawrence Berkeley National Laboratory, Berkeley, California 94720, United States;* ⓞ orcid.org/0000-0003-4195-310X

Complete contact information is available at:
https://pubs.acs.org/10.1021/jacs.1c10802

Author Contributions

R.M.P., C.M.A.-F., C.Y.R., and R.J.A. designed the research. R.M.P., M.C., S.T.-S., D.L., and P.D.A. performed experimental work. The manuscript was written through contributions of all authors. All authors have given approval to the final version of the manuscript.

Notes

The authors declare no competing financial interest.

ACKNOWLEDGMENTS

REFERENCES

(1) Alonso, E.; Sherman, A. M.; Wallington, T. J.; Everson, M. P.; Field, F. R.; Roth, R.; Kirchain, R. E. Evaluating rare earth element availability: A case with revolutionary demand from clean technologies. *Environ. Sci. Technol.* **2012**, *46* (6), 3406−3414.

(2) *Critical materials strategy*; US Department of Energy, 2010.

(3) Gupta, B.; Malik, P.; Deep, A. Solvent Extraction and Separation of Tervalent Lanthanides and Yttrium Using Cyanex 923. *Solvent Extr. Ion Exch.* **2003**, *21* (2), 239−258.

(4) Peppard, D.; Mason, G.; Maier, J.; Driscoll, W. Fractional extraction of the lanthanides as their di-alkyl orthophosphates. *J. Inorg. Nucl. Chem.* **1957**, *4* (5−6), 334−343.

(5) Elchuk, S.; Cassidy, R. Separation of the lanthanides on high-efficiency bonded phases and conventional ion-exchange resins. *Anal. Chem.* **1979**, *51* (9), 1434−1438.

(6) Kaur, H.; Agrawal, Y. Functionalization of XAD-4 resin for the separation of lanthanides using chelation ion exchange liquid chromatography. *React. Funct. Polym.* **2005**, *65* (3), 277−283.

(7) Anderegg, G. *Critical Survey of Stability Constants of EDTA Complexes: Critical Evaluation of Equilibrium Constants in Solution: Stability Constants of Metal Complexes*; Elsevier, 2013.

(8) Deblonde, G. J. P.; Mattocks, J. A.; Park, D. M.; Reed, D. W.; Cotruvo, J. A.; Jiao, Y. Selective and Efficient Biomacromolecular Extraction of Rare-Earth Elements using Lanmodulin. *Inorg. Chem.* **2020**, *59* (17), 11855−11867.

(9) Featherston, E. R.; Issertell, E. J.; Cotruvo, J. A. Probing Lanmodulin's Lanthanide Recognition via Sensitized Luminescence Yields a Platform for Quantification of Terbium in Acid Mine Drainage. *J. Am. Chem. Soc.* **2021**, *143* (35), 14287−14299.

(10) Lumpe, H.; Menke, A.; Haisch, C.; Mayer, P.; Kabelitz, A.; Yusenko, K. V.; Guilherme Buzanich, A.; Block, T.; Pöttgen, R.; Emmerling, F.; Daumann, L. J. The Earlier the Better: Structural Analysis and Separation of Lanthanides with Pyrroloquinoline Quinone. *Chem. Eur. J.* **2020**, *26* (44), 10133−10139.

(11) Caldwell, S. J.; Haydon, I. C.; Piperidou, N.; Huang, P.-S.; Bick, M. J.; Sjöström, H. S.; Hilvert, D.; Baker, D.; Zeymer, C. Tight and specific lanthanide binding in a de novo TIM barrel with a large internal cavity designed by symmetric domain fusion. *Proc. Natl. Acad. Sci. U. S. A.* **2020**, *117* (48), 30362.

(12) Mattocks, J. A.; Tirsch, J. L.; Cotruvo, J. A. Determination of affinities of lanthanide-binding proteins using chelator-buffered titrations. *Methods Enzymol.* **2021**, *651*, 23−61.

(13) Sára, M.; Sleytr, U. B. S-layer proteins. *J. Bacteriol.* **2000**, *182* (4), 859−868.

(14) Damiati, S.; Peacock, M.; Mhanna, R.; Søpstad, S.; Sleytr, U. B.; Schuster, B. Bioinspired detection sensor based on functional nanostructures of S-proteins to target the folate receptors in breast cancer cells. *Sens. Actuators, B* **2018**, *267*, 224−230.

(15) Ilk, N.; Egelseer, E. M.; Sleytr, U. B. S-layer fusion proteins—construction principles and applications. *Curr. Opin. Biotechnol.* **2011**, *22* (6), 824−831.

(16) Sára, M.; Pum, D.; Schuster, B.; Sleytr, U. B. S-layers as patterning elements for application in nanobiotechnology. *J. Nanosci. Nanotechnol.* **2005**, *5* (12), 1939−1953.

(17) Baranova, E.; Fronzes, R.; Garcia-Pino, A.; Van Gerven, N.; Papapostolou, D.; Péhau-Arnaudet, G.; Pardon, E.; Steyaert, J.; Howorka, S.; Remaut, H. SbsB structure and lattice reconstruction unveil Ca^{2+} triggered S-layer assembly. *Nature* **2012**, *487* (7405), 119−122.

(18) Bharat, T. A.; Kureisaite-Ciziene, D.; Hardy, G. G.; Yu, E. W.; Devant, J. M.; Hagen, W. J.; Brun, Y. V.; Briggs, J. A.; Löwe, J. Structure of the hexagonal surface layer on Caulobacter crescentus cells. *Nat. Microbiol.* **2017**, *2* (7), 1−6.

(19) Mann, V. R.; Manea, F.; Borys, N. J.; Ajo-Franklin, C. M.; Cohen, B. E. Controlled and Stable Patterning of Diverse Inorganic Nanocrystals on Crystalline Two-Dimensional Protein Arrays. *Biochemistry* **2021**, *60* (13), 1063−1074.

(20) Charrier, M.; Li, D.; Mann, V. R.; Yun, L.; Jani, S.; Rad, B.; Cohen, B. E.; Ashby, P. D.; Ryan, K. R.; Ajo-Franklin, C. M. Engineering the S-layer of Caulobacter crescentus as a foundation for stable, high-density, 2D living materials. *ACS Synth. Biol.* **2019**, *8* (1), 181−190.

(21) Vijayaraghavan, K.; Yun, Y.-S. Bacterial biosorbents and biosorption. *Biotechnol. Adv.* **2008**, *26* (3), 266−291.

(22) Nishitani, T.; Shimada, M.; Kuroda, K.; Ueda, M. Molecular design of yeast cell surface for adsorption and recovery of molybdenum, one of rare metals. *Appl. Microbiol. Biotechnol.* **2010**, *86* (2), 641−648.

(23) Valls, M.; Atrian, S.; de Lorenzo, V.; Fernández, L. A. Engineering a mouse metallothionein on the cell surface of Ralstonia eutropha CH34 for immobilization of heavy metals in soil. *Nat. Biotechnol.* **2000**, *18* (6), 661−665.

(24) Park, D. M.; Brewer, A.; Reed, D. W.; Lammers, L. N.; Jiao, Y. Recovery of Rare Earth Elements from Low-Grade Feedstock Leachates Using Engineered Bacteria. *Environ. Sci. Technol.* **2017**, *51* (22), 13471−13480.

(25) Park, D. M.; Reed, D. W.; Yung, M. C.; Eslamimanesh, A.; Lencka, M. M.; Anderko, A.; Fujita, Y.; Riman, R. E.; Navrotsky, A.; Jiao, Y. Bioadsorption of rare earth elements through cell surface display of lanthanide binding tags. *Environ. Sci. Technol.* **2016**, *50* (5), 2735−2742.

(26) Sturzbecher-Hoehne, M.; Ng Pak Leung, C.; D'Aléo, A.; Kullgren, B.; Prigent, A.-L.; Shuh, D. K.; Raymond, K. N.; Abergel, R. J. 3,4,3-LI(1,2-HOPO): In vitro formation of highly stable lanthanide complexes translates into efficacious in vivoeuropium decorporation. *Dalton Trans.* **2011**, *40* (33), 8340−8346.

(27) Abergel, R. J.; D'Aléo, A.; Ng Pak Leung, C.; Shuh, D. K.; Raymond, K. N. Using the Antenna Effect as a Spectroscopic Tool: Photophysics and Solution Thermodynamics of the Model Luminescent Hydroxypyridonate Complex [EuIII(3,4,3-LI(1,2-HOPO))]⁻. *Inorg. Chem.* **2009**, *48* (23), 10868−10870.

(28) Pallares, R. M.; Hébert, S.; Sturzbecher-Hoehne, M.; Abergel, R. J. Chelator-assisted high performance liquid chromatographic separation of trivalent lanthanides and actinides. *New J. Chem.* **2021**, *45* (32), 14364−14368.

(29) Wang, Y.; Deblonde, G. J. P.; Abergel, R. J. Hydroxypyridinone Derivatives: A Low-pH Alternative to Polyaminocarboxylates for TALSPEAK-like Separation of Trivalent Actinides from Lanthanides. *ACS Omega* **2020**, *5* (22), 12996−13005.

(30) Pallares, R. M.; An, D. D.; Deblonde, G. J. P.; Kullgren, B.; Gauny, S. S.; Jarvis, E. E.; Abergel, R. J. Efficient discrimination of transplutonium actinides by in vivo models. *Chemical Science* **2021**, *12* (14), 5295−5301.

(31) An, D. D.; Villalobos, J. A.; Morales-Rivera, J. A.; Rosen, C. J.; Bjornstad, K. A.; Gauny, S. S.; Choi, T. A.; Sturzbecher-Hoehne, M.; Abergel, R. J. 238Pu elimination profiles after delayed treatment with 3,4,3LI(1,2HOPO) in female and male Swiss-Webster mice. *Int. J. Radiat. Biol.* **2014**, *90* (11), 1055−1061.

(32) Abergel, R. J.; Durbin, P. W.; Kullgren, B.; Ebbe, S. N.; Xu, J.; Chang, P. Y.; Bunin, D. I.; Blakely, E. A.; Bjornstad, K. A.; Rosen, C. J.; Shuh, D. K.; Raymond, K. N. Biomimetic actinide chelators: an update on the preclinical development of the orally active hydroxypyridonate decorporation agents 3,4,3-LI(1,2-HOPO) and 5-LIO(Me-3,2-HOPO). *Health Phys.* **2010**, *99* (3), 401−407.

(33) Pallares, R. M.; Agbo, P.; Liu, X.; An, D. D.; Gauny, S. S.; Zeltmann, S. E.; Minor, A. M.; Abergel, R. J. Engineering Mesoporous Silica Nanoparticles for Targeted Alpha Therapy against Breast Cancer. *ACS Appl. Mater. Interfaces* **2020**, *12* (36), 40078−40084.

(34) Pallares, R. M.; An, D. D.; Tewari, P.; Wang, E. T.; Abergel, R. J. Rapid detection of gadolinium-based contrast agents in urine with a chelated europium luminescent probe. *ACS Sens.* **2020**, *5* (5), 1281−1286.

(35) Pallares, R. M.; Carter, K. P.; Zeltmann, S. E.; Tratnjek, T.; Minor, A. M.; Abergel, R. J. Selective Lanthanide Sensing with Gold Nanoparticles and Hydroxypyridinone Chelators. *Inorg. Chem.* **2020**, *59* (3), 2030−2036.

(36) Norville, J. E.; Kelly, D. F.; Knight, T. F.; Belcher, A. M.; Walz, T. Fast and easy protocol for the purification of recombinant S-layer protein for synthetic biology applications. *Biotechnol. J.* **2011**, *6* (7), 807−811.

(37) Charrier, M.; Ajo-Franklin, C. M. Engineering thermophilic microorganisms to selectively bind strategic metals in low temperature geothermal brines. *Proceedings of the 42nd Work on Geothermal Reservoir Engineering*, Standford, CA, February 13−15, 2017.

(38) Abergel, R. J.; D'Aléo, A.; Ng Pak Leung, C.; Shuh, D. K.; Raymond, K. N. Using the antenna effect as a spectroscopic tool: photophysics and solution thermodynamics of the model luminescent

hydroxypyridonate complex [EuIII (3,4,3-LI(1,2-HOPO))]⁻. *Inorg. Chem.* **2009**, *48* (23), 10868−10870.

(39) Deblonde, G. J.; Sturzbecher-Hoehne, M.; Abergel, R. J. Solution thermodynamic stability of complexes formed with the octadentate hydroxypyridinonate ligand 3,4,3-LI(1,2-HOPO): a critical feature for efficient chelation of lanthanide (IV) and actinide (IV) ions. *Inorg. Chem.* **2013**, *52* (15), 8805−8811.

(40) Sturzbecher-Hoehne, M.; Choi, T. A.; Abergel, R. J. Hydroxypyridinonate complex stability of group (IV) metals and tetravalent f-block elements: The key to the next generation of chelating agents for radiopharmaceuticals. *Inorg. Chem.* **2015**, *54* (7), 3462−3468.

(41) Dimmock, P. W.; Warwick, P.; Robbins, R. A. Tutorial review. Approaches to predicting stability constants. *Analyst* **1995**, *120* (8), 2159−2170.

(42) Cotton, S. *Lanthanide and actinide chemistry*; John Wiley & Sons, 2013.

(43) Jarmoskaite, I.; AlSadhan, I.; Vaidyanathan, P. P.; Herschlag, D. How to measure and evaluate binding affinities. *eLife* **2020**, *9*, e57264.

📖 Recommended by ACS

Mn²⁺ Bispidine Complex Combining Exceptional Stability, Inertness, and MRI Efficiency

Daouda Ndiaye, Éva Tóth, *et al.*

NOVEMBER 29, 2022

JOURNAL OF THE AMERICAN CHEMICAL SOCIETY   READ 🗗

Size Selective Ligand Tug of War Strategy to Separate Rare Earth Elements

Katherine R. Johnson, Santa Jansone-Popova, *et al.*

JANUARY 25, 2023

JACS AU   READ 🗗

In Vivo Uranium Decorporation by a Tailor-Made Hexadentate Ligand

Bin Chen, Shuao Wang, *et al.*

JUNE 14, 2022

JOURNAL OF THE AMERICAN CHEMICAL SOCIETY   READ 🗗

Chelating Rare-Earth Metals (Ln³⁺) and ²²⁵Ac³⁺ with the Dual-Size-Selective Macrocyclic Ligand Py₂-Macrodipa

Aohan Hu, Nikki A. Thiele, *et al.*

AUGUST 01, 2022

INORGANIC CHEMISTRY   READ 🗗

Get More Suggestions >